EXTRACTION OF URBAN ELEVATION MODELS FROM HIGH RESOLUTION INTERFEROMETRIC SAR IMAGES

C. Tison, GET-Télécom Paris- CNRS UMR 5141, Paris, France and CNES, Toulouse, France
F. Tupin, GET-Télécom Paris- CNRS UMR 5141, Paris, France
H. Maître, GET-Télécom Paris- CNRS UMR 5141, Paris, France

Abstract

This article presents a method for digital elevation model extraction from high resolution interferometric SAR images over urban areas. Our algorithm, based on the use of a unique SAR interferometric couple, processes each building separately in order to retrieve the best enclosing polygonal shape, the layover area and the ground/wall dihedral structures. The ground level is extracted in parallel. In this paper, we focus on building height extraction. The specific steps are described in the paper and illustrated by examples on real data.

1 Introduction

SAR images over urban areas provide useful information on the density of houses, the orientation of the streets, etc., all pieces of information which are of highest importance for equipment planning, natural risk prevention or defence. Furthermore, with interferometric SAR data, the height of each illuminated point of the scene may be retrieved. The recent improvement of the SAR image resolution enables to focus on man-made structures, such as buildings. Thus a new challenge arises with computing of urban area DEM[1] from interferometric SAR data.

Different processes have already been proposed to extract building heights through SAR interferometry: shape from shadow (Bolter [1]), machine vision (Gamba et al. [2]), stochastic geometry (Quartulli et al. [3]) or segmentation based algorithm (Soergel et al. [4]). We have chosen to use a segmentation based algorithm as it uses only one track (versus at least two, for the shape from shadow method) and have prior no restriction on height or geometry of the buildings (machine vision is essentially efficient for high large isolated buildings). In a recent paper, we proposed an efficient classification method [5], which enables to discriminate ground and building pixels in high resolution SAR images. Relying on this result, the approach presented in this paper, deals then with each building separately and it is based on primitive extraction (such as ground/wall dihedral structures, layovers, etc.).

This paper is dedicated to the building height extraction part. The other parts of the global process are quickly described. In the first Section, the limits and objectives are exposed. The second Section describes the process. The analysis of some results concludes the paper.

2 SAR interferometry and urban areas

2.1 From phase to height

SAR interferometry relies on the phase difference of two correlated signals (s_1 and s_2). The L-look interferometric phase Φ and the corresponding coherence ρ are defined by ([6]):

$$\rho e^{j\Phi} = \frac{\left(\sum_{n=1}^{L} s_1(n)\right)\left(\sum_{n=1}^{L} s_2^*(n)\right)}{\sqrt{\sum_{n=1}^{L} |s_1(n)|^2 \sum_{n=1}^{L} |s_2(n)|^2}} \quad (1)$$

Relative height h and interferometric phase are linked by the following relation:

$$h = \frac{\lambda}{2\pi} \frac{R\sin(\theta)}{B_\perp} \Phi \quad (2)$$

with R the mean distance between sensors and the target, $B_\perp$ the orthogonal projection of the baseline (distance between the two sensors) on the perpendicular direction to the propagation axis, λ the wavelength and θ the viewing angle.

This study is made for airborne high resolution sensors, where the ambiguity altitude is high regarding the height variations in the urban scene (for instance 170 m versus less than 25 m, in our case). A phase unwrapping stage should thus not be done.

2.2 Problems and objectives

Even if Equation 2 states a very simple link between phase and height, the retrieval of DEM from interferometric phases is limited both by the intrinsic properties of SAR signals (layover, shadow) and the complex geometry of urban areas.

It has been shown [7] that a large part of the urban scene is contained in layover and shadow areas, where height information seems completely lost. In layovers, the interferometric phase is made of a combination between ground, wall and roof responses. An experimental analysis proved that no simple rule points out which term is dominant in the resulting phase. It strongly depends on the materials and the geometrical parameters. As a consequence, these areas should be detected and not used to compute the height of the buildings when possible.

A close analysis of the images underlines several aspects to be respected for the 3D process:

- the identification of layover areas,

- the extraction of ground/wall dihedral structures,

- the retrieval of the global building shape,

- the extraction of the roof shape.

Classification is thus required to discriminate ground and man-made pixels. Indeed these two large groups should not be processed in a same way because they deeply differ in nature and geometry. They are thus processed with separate algorithms adressing each kind of surfaces. The global
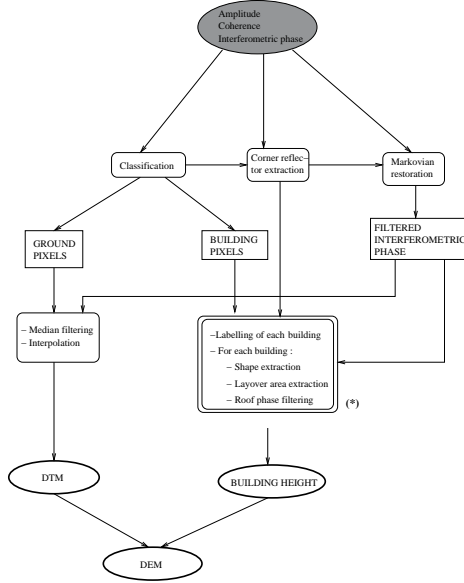
---

[1]DEM=Digital Elevation Model

Figure 1: *Graph of the global approach for DEM computing. The part (*) is detailed in this article.*

approach and the algorithms are described in the next section.

3   Description of the DEM extraction

This section is dedicated to an overview of the method and an explanation of the whole framework. The different modules are detailed in Section 4.

3.1   Global approach

The global approach is summarized in Figure 1. Illustrations are made in Section 5 with real data. The three first steps (classification, corner reflector extraction and interferometric phase restoration) are processed whatever the class of pixel. Then, a discrimination between ground and man-made pixels is made (Sections 3.3 and 4). Since this work is focused on man-made pixels, the other parts are briefly evocated. The final DEM is obtained by merdging the ground elevation and the building elevations.

3.2   Preliminary process
3.2.1   Classification

In recent articles [5, 8], a Markovian classification method has been proposed for SLC amplitude images. It is improved in a fusion algorithm [9] by taking into account the interferometric phase and the coherence map. Finally six classes are deduced: ground, vegetation, dark roof, medium roof, light roof and shadow.

3.2.2   Ground/wall dihedral structure extraction

The extraction of the ground/wall dihedral structures is deeply needed to localize layovers in the buildings. The algorithm, proposed in [12], enables us to extract linear structures from the amplitude image. Then, constraints on the interferometric phase value (close to a ground reference Φ_{ref}), on the orientation of the structures relative to the track orientation ($\Delta\alpha$) and on its size (nb_{min} pixels) make a selection between them. Finally a Radon transform

provides a unique long line for each ground/wall dihedral structure; a matching with the classification eliminates the parts of the lines which do not belong to a building.

This module requires some experimental adjustments to find the best parameters Φ_{ref}, $\Delta\alpha$ and nb_{min} regarding the characteristics of the scene to reconstruct.

3.2.3   Interferometric phase restoration

A constrained restoration of the interferometric phase is made in order to reduce the interferogram noise level. A Markovian restoration with implicit edge preserving function derived from [10, 11] is used, which enables to keep the discontinuities associated with building borders and ground/wall dihedral structures.

Once the classification is made, the ground and building pixels are separated and processed in parallel.

3.3   Ground level retrieval

The pixels, which are classified as ground or low vegetation (grass for instance), are used to compute the DTM[2]. As a smooth result is required, a median filter is applied on the selected pixels. Then a linear interpolation is performed to cover the entire scene.

4   Building height retrieval

In this section, all the steps of the building height computation are detailed.

4.1   Raw building shape extraction

The pixels of presumed buildings are deduced from the classification. But it may give connected area for separate buildings of different heights (twin houses for instance) and a label, for each building, is thus required. A Canny edge detector is thus applied, on the restored interferometric phases of the areas, which have been previously detected as buildings. From this result, a label map is computed in order to identify connected parts of equal height buildings.

4.2   Building shapes
4.2.1   Principle

The building raw shapes, which are given by the labeled areas, are noisy and contain holes. Approximations by polygonal shapes are thus needed. Indeed polygons are the most basic and common shape to describe buildings. A region based active contour, inspired from the CASP algorithm [13], is used. In this algorithm, contours are defined by nodes, the number of which increases at each step. This approach provides a global framework to estimate polygonal active contours. The same optimization algorithm is used as in [13] but with a different energy term. The simplification in energy computation proposed in [13] cannot apply since energy flux is not conserved in this case.

4.2.2   Energy function

The energy function of the contour C is defined from the original raw shape B of the buildings (given by the step

---

[2]DTM = Digital Terrain Model

of Paragraph 4.1) and the interferometric phase.

$$U(C) = (1 - \beta)U_\Phi(C) + \beta U_{shape}(C) \qquad (3)$$

$$U_\Phi(C) = \sum_{t \in S_C} \frac{(\Phi_t - \mu_B)^2}{2\sigma_B^2} \qquad (4)$$

$$U_{shape}(C) = \left| \frac{\omega card(S_C - S_C \cap B) + card(B - S_C \cap B)}{2} \right|^2 \qquad (5)$$

with B and S_C the sets of pixels of the original and polygonal shapes of the buildings, μ_B and σ_B are the mean and standard deviation values of the phase of the original building (B), β is a weight between the two energy terms and ω a weight between pixels of the two kinds of areas (S_C or B) which do not belong to $B \cap S_C$. The velocity function of the energy $U(C)$, defined as the derivates of U over the surface, cannot be explicit. Instead, the criterion is numerically estimated for each contour C with Equations 4 and 5. The most accurate contour is the one which minimizes the energy function U.

4.2.3 Optimization algorithm

The minimization of U is obtained using an iterative algorithm. Each step corresponds to a number of nodes n_{node}. Then, for n_{node} from 4 to n_{max}, do:

- search the optimal polygonal contour for n_{node} nodes. During N_{it} iterations:

  - randomly choose the node to be moved,
  - randomly choose, within a predefined interval $[-\delta, +\delta]$, the displacement of the node in range and azimuth,
  - compute the energy U,
  - accept or not the node move depending if it decreases or not the energy.

- add two new nodes only if the criterion $(C1)$ is not true, where $C1$ stands for:

$$(C_1) : \frac{U_{shape}}{card(B)} < th_1 \qquad (6)$$

If (C1) is true, the algorithm stops. The nodes are added on the sides which are the farest from the original shape.

The values of the parameters are, by experiment: $n_{max} = 10$, $\delta = 4$, $N_{it} = 6000$, $th_1 = 0.17$, $\omega = 2$ and $\beta = 0.6$. Note that the number of iterations N_{it} should be large enough to ensure convergence of the optimization algorithm. It is initialized by the quadrilateral bounding box of the original shape.
Now the building shape designs the polygonal one.

4.3 Layover identification

For each building associated with a ground/wall dihedral structure, the layover is detected as the area at the left of the structure (the radar platform is assumed to fly on the left of the images).

4.4 Roof phase filtering

For each building, the assumption of flat roofs is made. This hypothesis is, of course, very restrictive and should be improved in the future. Gamba et al. [2] proposed to model each roof by several planes instead.

When a dihedral structure is associated with a building, there are two main cases: either the roof is splitted into layover and pure roof parts or it is pure layover. For this last case, the presence of corner reflector is ignored and the roof pixels are processed as if there is no layover.

First, when only a part of the roof corresponds to a layover area, the mean of the interferometric phase is computed on the parts which are layover free and belong to the original raw shape. This value stands for the roof interferometric phase of the polygonal shape. When a building contains more than one single ground/wall dihedral structure, a phase value is computed for each part of the roof associated with a corner. In this case, the roof is splitted into different parts, which enables to retrieve more complex architectures. The mean of the interferometric phase on each ground/wall dihedral structure is associated to it.

Secondly, in all the other cases, the mean on the interferometric phase is computed taking into account all the roof pixels belonging to the original raw shape. But it may give, in many cases, a biased value (see Section 2.2).

Then the height of each pixel is obtained by Equation 2, providing results in the slant range geometry. Projection to a cartographic geocoding is a further step of work.

5 Results on real data

5.1 The data

We work on an X-band high resolution interferometric dataset over the French city of Dunkerque (North of France). The sensor is RAMSES. It provides an interferogram of six looks, the resolution of which is about 1.5 meters in range and azimuth.

5.2 Isolated buildings

An area with isolated buildings with a large panel of heights is extracted. The amplitude and corresponding classification are illustrated on Figure 2. Figures 3 and 2 are the results of the different modules described in Sections 3 and 4. The DEM is presented on Figure 4. The DTM contains some artifacts near the buildings or on small areas: they are due to few misclassified pixels and can be corrected by identifying the bumps and iterating the process. Anyway, the global structures of the scene is well retrieved and the major buildings are reconstructed with appropriate shapes.

5.3 Comparison to ground truth

A ground truth (©IGN) is available on this area. The mean value of each building of this database is compared to the one retrieved from the interferogram (Table 1). The computed height is not exact for some buildings. But record of buildings by increasing height is exactly the same in ground truth and in the interferometric DEM, which proves that results are very coherent regarding the reality.
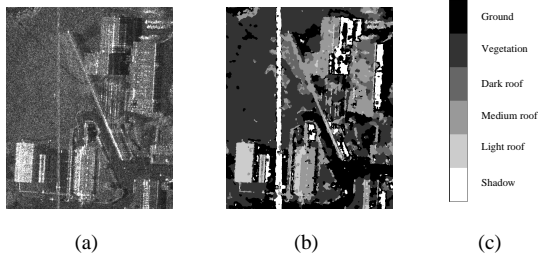
(a)   (b)   (c)

Figure 2: *Amplitude (a) and corresponding classification(b) for isolated building area (Bayard district in Dunkerque)*

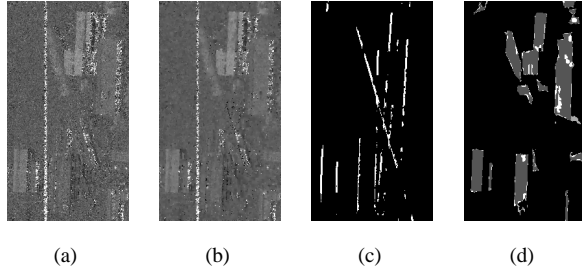(a)   (b)   (c)   (d)

Figure 3: *Original 6-looks interferometric phase (a), restored interferometric phase (b), mask of the ground/wall dihedral structures (c) and polygonal building shapes superimposed with original shape (d) for isolated building area.*

6 Conclusion

We proposed a method for urban height extraction from high resolution SAR interferometry. Our method exploits only an interferometric SAR couple. On isolated buildings, even with small elevation, results are very good when shapes are not too complex. If the complexity of the buildings increases, the simplification made by the active contour is not very appropriate and the result is less accurate than hopped. But the global shape of the scene is retrieved, showing the usefulness of interferometry on urban areas. Further works are the adding of the trees, the projection from slant range to ground range geometry. The merge with optical data is also a future research axis to improve
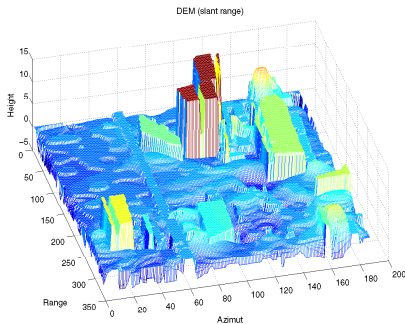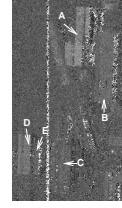

Figure 4: *DEM of isolated building area in meters and slant range geometry.*

Table 1: *Comparison between ground truth (©IGN) and estimated DEM. A mean height is given for each building.*

Building	Ground truth	DEM
A	14	13
B	5	5
C	5	3
D	9	6
E	4	3

the building shape detection.

7 References

[1] R. Bolter, "Reconstruction of man-made objects from high resolution SAR images," in *IEEE Aerospace Conference*, vol. 3, Mar. 2000, pp. 287–292.

[2] P. Gamba, B. Houshmand, and M. Saccani, "Detection and extraction of buildings from interferometric SAR data," *IEEE Transactions on Geoscience and Remote Sensing*, vol. 38, no. 1, pp. 611–617, Jan. 2000.

[3] M. Quartulli and M. Dactu, "Bayesian model based city reconstruction from high resolution ISAR data," *IEEE/ISPRS Joint Workshop on Remote Sensing and Data over Urban Areas*, Nov. 2001, rome.

[4] U. Soergel, K. Schuls, U. Thonnessen, and U. Stilla, "3D-visualization of interferometric SAR data," in *EUSAR 2000*, May 2000, pp. 305–308.

[5] C. Tison, J.-M. Nicolas, and F. Tupin, "Classification of X-band high resolution SAR images over urban areas: Markovian segmentation using Mellin transform," in *2nd GRSS/ISPRS Joint Workshop on Remote Sensing and Data Fusion over Urban Areas*, Berlin, Germany, May 2003, pp. 110–114.

[6] E. Rodriguez and J. Martin, "Theory and design of interferometric synthetic aperture radars," *IEE proceedings - F*, vol. 139, no. 2, Apr. 1992.

[7] U. Stilla, U. Soergel, and U. Thoennessen, "Potential and limits of InSAR data for building reconstruction in built-up areas," *ISPRS Journal of Photogrammetry and Remote Sensing*, pp. 113–123, May 2003.

[8] C. Tison, J.-M. Nicolas, and F. Tupin, "Accuracy of Fisher distributions and log-cumulant estimation in a markovian segmentation of high resolution SAR images over dense urban areas," in *IGARSS'03*, vol. 3, July 2003, pp. 1999–2001.

[9] X. Descombes, "A fission and fusion markovian approach for multi-channel segmentation," in *IGARSS'95*, vol. 1, 1995, pp. 124–126.

[10] D. Geman and G. Reynolds, "Constrained restoration and the recovery of discontinuities," *IEEE Transactions on Pattern Analysis and Machine Intelligence*, vol. 14, no. 3, pp. 367–383, 1992.

[11] P. Charbonnier, L. Blanc-Féraud, G. Aubert, and M. Barlaud, "Deterministic edge-preserving regularization in computed imaging," *IEEE Transactions on Image Processing*, vol. 6, no. 2, pp. 298–311, 1997.

[12] F. Tupin, H. Maître, J.-F. Mangin, J.-M. Nicolas, and E. Pechersky, "Detection of linear features in SAR images: application to road network extraction." *IEEE Transactions on Geoscience and Remote Sensing*, vol. 36, no. 2, pp. 434–453, Mar. 1998.

[13] C. Chesnaud, P. Réfrégier, and V. Boulet, "Statistical region snake-based segmentation adapted to different physical noise models," *IEEE Transactions on Pattern Analysis and Machine Intelligence*, vol. 21, no. 11, pp. 1145–1157, Nov. 1999.